Original paper

Clinical analysis of tethered cord syndrome and gene expression profiling of wound healing surgery

Rafał Staszkiewicz[1,2], Dorian Gładysz[1], Edward Golec[3], Wiesław Marcol[4,5], Beniamin O. Grabarek[1,2]

[1]Department of Neurosurgery, 5th Military Clinical Hospital with the SP ZOZ Polyclinic, Krakow, Poland
[2]Department of Histology, Cytophysiology and Embryology, Faculty of Medicine in Zabrze, Academy of Silesia in Katowice, Poland
[3]Department of Rehabilitation in Orthopaedics, Faculty of Motor Rehabilitation, Bronisław Czech University of Physical Education, Krakow, Poland
[4]Department of Physiology, School of Medicine, Medical University of Silesia, Katowice, Poland
[5]Department of Neurosurgery, Provincial Specialist Hospital No. 2, Jastrzebie-Zdroj, Poland

Adv Dermatol Allergol 2023; XL (1): 78–86
DOI: https://doi.org/10.5114/ada.2022.120001

Abstract

Introduction: The method to prevent progression of symptoms in tethered cord syndrome (TCS) is neurosurgery. However, postoperative wound healing is a lengthy process and is hindered by the release of cerebrospinal fluid (CSF) through the wound. To the best of the authors' knowledge, there is no study evaluating the changes in the expression of factors involved in the wound healing process after neurosurgery for TCS.
Aim: To clinically analyse 2 cases of TCS and evaluate the change in expression of selected genes during the post-operative wound healing process.
Material and methods: Determination of TCS in two adult patients (woman, aged 26 years; man, aged 53 years) was based on magnetic resonance imaging (MRI). After confirming the initial diagnosis, a neurosurgical procedure was performed to remove the intrathecal spreading adipoma and transect the medullary terminal thread in patients. In the postoperative period, impaired wound healing was noted as a result of CSF secretion through the surgical wound.
Results: Molecularly, there was an increase in expression of all genes assessed in skin biopsy specimens compared to skin samples. Impaired postoperative wound healing after neurosurgery for TCS is expected due to CSF leakage through the surgical wound. The greatest changes were noted for metalloproteinases (MMPs) and four isoforms (A–D) of vascular endothelial growth factor A-D (VEGF-A-D; $p < 0.05$).
Conclusions: Changes in the expression of our selected genes can be used to monitor and predict the process of wound healing and scar formation, which occurred in our cases at 19 and 20 days after surgery.

Key words: wound healing, gene, tethered cord syndrome, transforming growth factor β, RTqPCR, spinal stenosis, surgical treatment.

Introduction

Tethered cord syndrome (TCS) is any low position of the spinal conus below the L3 vertebral body caused by a thickened, shortened terminal strand. The definition has been expanded to include any low position of the spinal cord due to causes such as fatoma, postoperative scarring changes, or adhesions resulting from a history of trauma [1, 2]. TCS results from abnormal embryogenesis during the process of retrograde differentiation of a set of cells of the caudal region. Previously formed caudal cells undergo directed necrosis and only the terminal niche, cuneiform ligament, and terminal conchae remain until 11 weeks of foetal life. Inappropriate cell necrosis gives rise to a thickened terminal nematode and/or terminal thread lipoma [3–6]. Symptoms and neurological deficits in TCS are caused by hypoxia in the distended medulla due to vascular insufficiency. The most common symptoms are back pain, lower extremity weakness, sphincter dysfunction, and sciatica-type pain. In addition to neurological symptoms, the following may be present: skin stigmata, foot deformity, scoliosis of the thoracic

Address for correspondence: Rafał Staszkiewicz MD, PhD, 5th Military Clinical Hospital with the SP ZOZ Polyclinic, Krakow, Department of Histology, Cytophysiology and Embryology, Faculty of Medicine, Academy of Silesia, Zabrze, Poland, e-mail: rafalstaszkiewicz830@gmail.com
Received: 20.07.2022, **accepted:** 18.08.2022.

and lumbar spine, muscular atrophy of the lower extremities [7–9]. According to O'Connor, by 2019, a total of only 730 cases of TCS in adults have been described [2].

In spite of the identical radiological picture and similar pathophysiology, the clinical presentation of TCS differs between children and adults. In children, common symptoms include foot deformity, progressive scoliosis, gait disturbances, sphincter disorders, and trophic ulcers of the lower extremities, which are rare in adults [10–12]. In adults, however, the most common symptom is pain, which rarely accompanies this disease diagnosed in childhood. In contrast to adults, growth acceleration is an important factor exacerbating the disease in children, whereas in adults the symptoms are exacerbated by trauma, lumbar spondylosis, lumbar discopathy, and degenerative spinal stenosis [13, 14]. It has been proposed to divide patients with TCS into four groups [15]:

1. True TCS (medullary cone located low, accompanying small adipoma, thickened terminal niche);
2. Partial TCS (spinal cord dysfunction caused by cord tension, for example, as a result of trauma, without an anatomical low-lying cord with a full set of characteristic symptoms);
3. Non-traction-induced conditions with symptoms similar to TCS;
4. Medullary cleft in the medullary conus or extensive myelomeningocele in the superior lumbar region (neurological symptoms are due to medullary cleft or dysgenesis in the superior lumbar region; there are no active neurons in the conus).

Of these, the first group is the most promising, but full recovery is doubtful [15].

The treatment of choice for TCS is neurosurgical transection of the spinal cord end thread. Unfortunately, the healing process is hindered due to the release of cerebrospinal fluid (CSF) through the surgical wound [16–19]. The key factors in the wound healing process are transforming growth factor β (TGF-β) superfamily [20, 21], four isoforms (A–D) of vascular endothelial growth factor (VEGF) [22], tumor necrosis factor α (TNF-α) [23], extracellular matrix metalloproteinases (MMPs) [24, 25], fibroblast growth factors (FGF) or interleukins (ILs), and genes encoding collagen (COL) proteins [26]. To date, to the best of the authors' knowledge, there has been no study evaluating the changes in the expression of factors involved in the wound healing process after neurosurgery for TCS.

Aim

The aim of this study was to clinically analyse 2 cases of TCS and evaluate the change in expression of selected genes during the postoperative wound healing process.

Material and methods

Case 1

The patient, aged 28 years, was admitted to the Neurosurgery Department due to lumbosacral (L/S) pain radiating to lower limbs and sphincter disturbances with urinary and faecal incontinence. On admission, she also complained of progressive weakness of lower limbs for about a year. Neurological examination revealed weakness of lower limbs in dorsiflexion and plantar flexion of the foot, bilateral abolition of Achilles tendon reflexes, and sensory disturbances of bifurcation type affecting S1, S2 and, S3 roots and the perineal area.

Magnetic resonance imaging (MRI) of the lumbosacral (L/S) spine

An MRI scan (1.5 T) showed a low-terminal spinal cone at the S2 level with a thickened terminal nerve, as well as a lesion with a high signal at T2 time, which corresponds to an intramedullary adipoma spreading into the subcutaneous tissue through the unattached L5 arch. The image corresponding to the first type of TCS can be observed in Figure 1.

Surgery and early postoperative period

The patient was operated under general endotracheal anaesthesia in the supine position. The skin was incised in the lumbosacral region at 7 cm over the spinous process of L5 and the sacral crest. After removal of the spinous processes of the L5 and S1 vertebral arches, the operating microscope and microsurgical technique were used. The meningeal sac was incised above the site of the adipose tissue exit, and the entire mass of the adipose tissue, 5 cm in diameter with the spinal nerve roots passing through it, was visualized. The adipose had spread beyond the spinal canal into the adipose tissue. The tumour was removed subtotally. Complete resection was not possible because of the overgrowth of the spinal nerves and the consequent risk of their damage. The entoptic thread visible under the operating microscope was thicker than the nerve roots and had a white iridescent colour with connective tissue fibres visible on its surface. After cutting the terminal thread, a reduction in the tension of the nerve elements was obtained. In order to verify the nerve structures, intraoperative monitoring was used: sensory and motor evoked potentials (SSEP) and electromyogram (EMG). The 12 mm long subcutaneous steel electrodes were used for SSEP stimulation and monitoring of lower limbs. EMG was studied using 25 mm electrodes placed in the quadriceps femoris, tibialis anterior, and gastrocnemius muscles, bilaterally. Electrodes were also placed bilaterally in the external rectus sphincter muscles. An electrode was placed on the Foley catheter to monitor the external urethral sphincter. Bipolar stimulation was applied during preparation to assess the functionality of the neural tissue. The potentials evoked by manipulation or stimulation of the monitored nerve roots were processed by the neuromonitoring system into sound signals heard and interpreted by the surgeon. The patient had significant improvement in lower limb mobility and sphincter function. There was minimal improvement in sensation. The pain in the lumbar region remained unchanged. The early postoperative period was

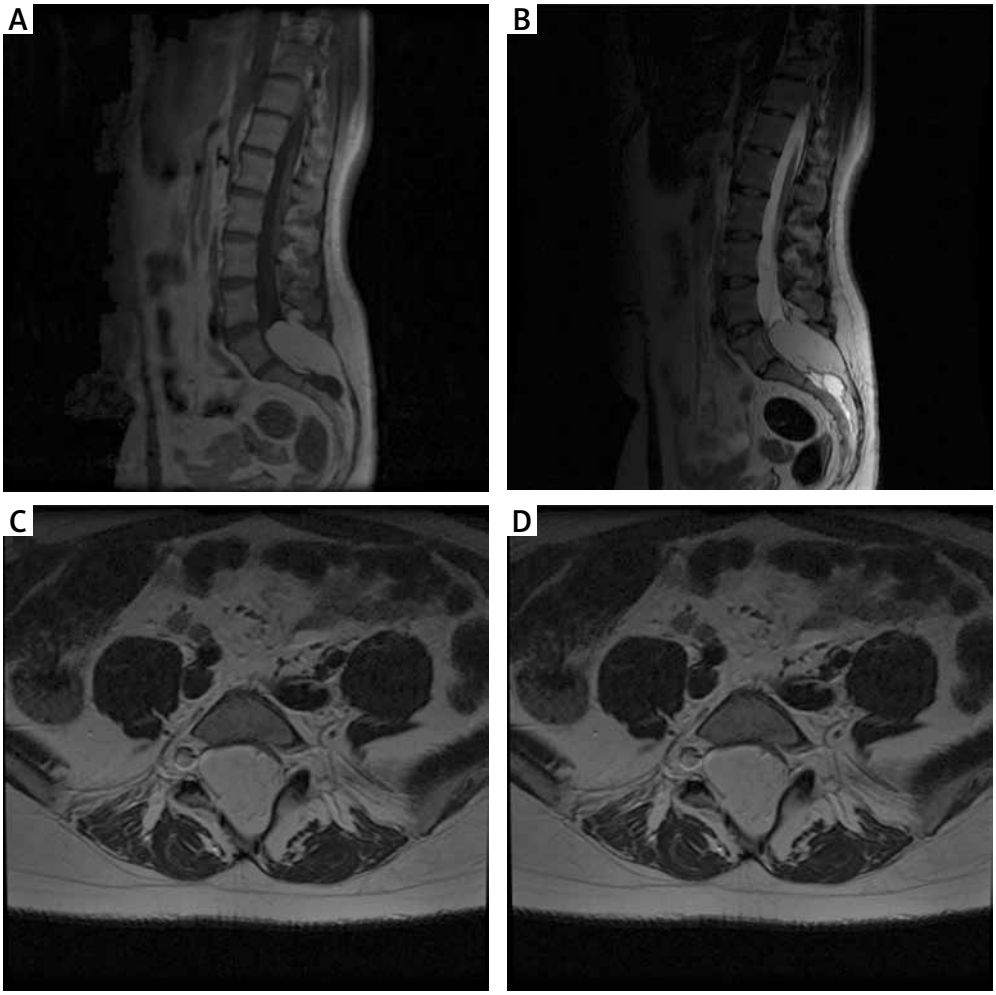

Figure 1. Pre-operative MRI examination of the first patient. **A** – T1 FSE S time with contrast; visible end-striatal fatoma and non-union of L5 and S1 arch. **B** – T2 time. **C** – axial sections at T2 time; widening of the spinal canal, filled with adipoma. **D** – axial sections at T1 time with contrast; the tumour shows no contrast enhancement

complicated by a fluid cyst, palpable subcutaneously and visible on postoperative MRI (Figure 2). The CSF collection was treated with several punctures and evacuation of the fluid. The patient was discharged on postoperative day 14. A scar at the surgical wound site developed 20 days after surgery.

Late postoperative period

The patient had significant improvement in lower limb mobility and sphincter function. There was minimal improvement in sensation. The pain in the lumbar region remained unchanged. The patient was consulted on an outpatient basis 12 months after the surgical treatment. She did not report any recurrence of symptoms and the therapeutic effect remained good. MRI examination showed healed surgical area and subtotally removed adipose tissue (Figure 3).

Case 2

A 53-year-old patient was admitted to the Department of Neurosurgery because of urinary incontinence (neurogenic bladder) unsuccessfully treated in the urology outpatient clinic. The patient also complained of low back pain, which had been exacerbated after exertion for about 14 months. The neurological examination revealed weakness of lower limbs in dorsal and sole flexion of the foot, bilateral abolition of Achilles tendon reflexes, sensory disturbances of bifurcation type affecting S1, S2, S3 roots, and difficulties in walking,

MRI examination of the L/S spine

MRI (1.5 T) showed a thickened terminal strand with a low-lying spinal cone at the S2 level and an accompanying terminal strand fatoma, which argues for the first type of TCS (true TCS, Figure 4).

Figure 2. MRI examination in the early postoperative period in the first patient. **A** – T2-weighted postoperative study with visible fluid cyst. **B** – T1-weighted contrast-enhanced MR study with visible cyst and partially removed adipoma. **C** – Axial sections of T2-weighted contrast-enhanced MR study; fluid collection and degree of resection visible

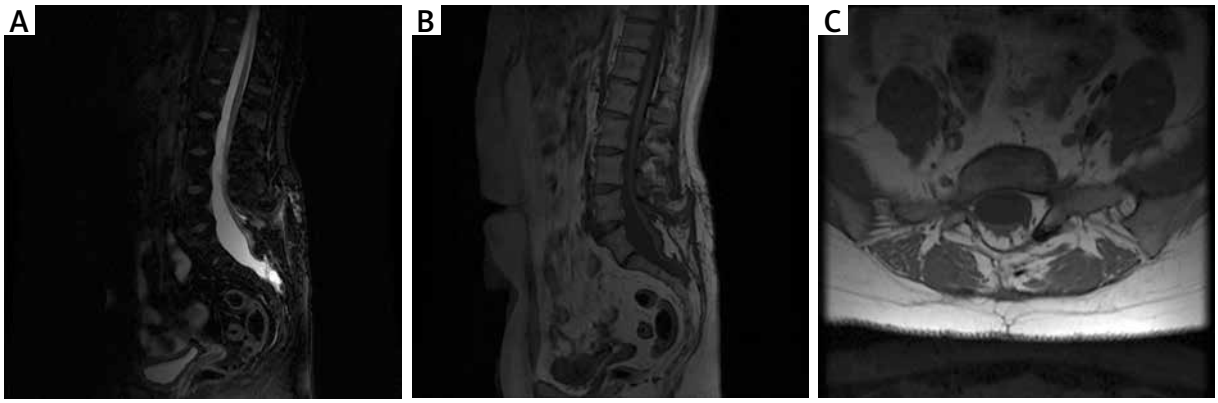

Figure 3. MRI scan at 12 months after surgery in the first patient. **A** – T2-weighted MR imaging with a healed surgical approach area. **B** – T1-weighted MR imaging with variable flip; a properly healed surgical approach area. **C** – T1-weighted MR imaging, axial sections; healed wound with the visible laminectomy site

Figure 4. Preoperative MRI examination of the second patient. **A** – T1-weighted study showing end-strand adipose and end cone at L5-S1. **B** – T1-weighted study, coronary sections; visible ratio of the fatoma to the terminal strand. **C** – axial sections at T2 time; fat pad filling the vertebral canal with visible end thread

Surgery and early postoperative period

The patient was operated under general endotracheal anaesthesia. During the surgery, neuromonitoring was used: evoked sensory-motor potentials from the lower limbs and EMG of the anal sphincter, urethra, and muscle groups supplied by the L2–S2 spinal nerve roots as in the previously described case. The skin was incised in the lumbosacral region at 7 cm over the spinous process of

L5 and the sacral crest. After dehiscence of the spinal extensor muscles, the sacrum and L5 vertebral arch were visualized. A partial laminectomy of the lower part of the L5 arch and laminectomy of S1 to S3 was performed. The fat pad was separated from the dura mater, resulting in a reduction in tension of the terminal strand. The end-to-end transection was abandoned due to the decreased tension of the nerve elements after separation of the adipose tissue. The adipose tissue was partially removed because of the close proximity of the nerve roots and high risk of their damage during the removal. Intraoperative monitoring was used during surgery as in the previous case. The patient's pain decreased, with no significant effect on sphincter control. Similar to the previous case, difficulties in postoperative wound healing were noted due to the fluid cyst. The patient was discharged on postoperative day 14. A scar at the surgical wound site developed 19 days after surgery.

Late postoperative period

Ten months later, during another outpatient visit, MRI was performed (Figure 5). Clinically, the patient's condition had improved since discharge from the neurosurgery department, pain was significantly reduced, and sphincter function did not deteriorate.

Microbiological evaluation of cerebrospinal fluid

Standardly used media, that is, blood agar and chocolate agar, were used for microbiological evaluation of the collected CSF.

Samples

Biopsy specimens of skin tissue approximately 3 mm in diameter over the spinous process of L5 and the sacral crest were taken during surgery (time 0) and then on days 1, 7, and 10, postoperatively, from both patients during CSF aspiration. Controls were skin tissue biopsy specimens obtained from the same patients at the same time intervals from the gluteal region. Samples were preserved in RNAlater solution (Thermo Fisher Scientific, Waltham, MA) and stored at –20°C until molecular analysis.

Molecular analysis

Total ribonucleic acid (RNA) was isolated from skin samples using Trizol reagent (Invitrogen Life Technologies, Carlsbad, CA, USA) according to the manufacturer's recommendation. RNA extracts were then evaluated qualitatively (electrophoresis in 1% agarose gel with ethidium bromide) and quantitatively by spectrophotometry. The expression pattern of the genes evaluated was determined by real-time reverse transcription polymerase chain reaction (RTqPCR) using two endogenous controls: β-actin (ACTB) and glyceraldehyde-3-phosphate dehydrogenase (GAPDH). The thermal condition of RTqPCR was as follows: reverse transcription (45°C for 10 min), activation of the polymerase (95°C for 2 min), and 40 cycles including denaturation (95°C for 5 s), annealing (60°C for 10 s), and elongation (72°C for 5 s). We used the SensiFAST™ SYBR No-ROX One-Step Kit, (Bioline, London, UK). The nucleotide sequence of the primers is shown in Table 1. All the reactions were performed in triplicate in 96-well plates. Changes in gene expression over time were presented using the relative gene expression score method ($2^{-\Delta\Delta CT}$ method) as Fold Change (FC).

Statistical analysis

Statistical analysis was performed using the Statistica 13 PL program (StatSoft, Cracow, Poland) at a statistical significance threshold of $p < 0.05$. The Kruskal-Wallis analysis of variance followed by Dunn's post-hoc test were used to determine statistically significant changes in the expression of each gene during the observation period.

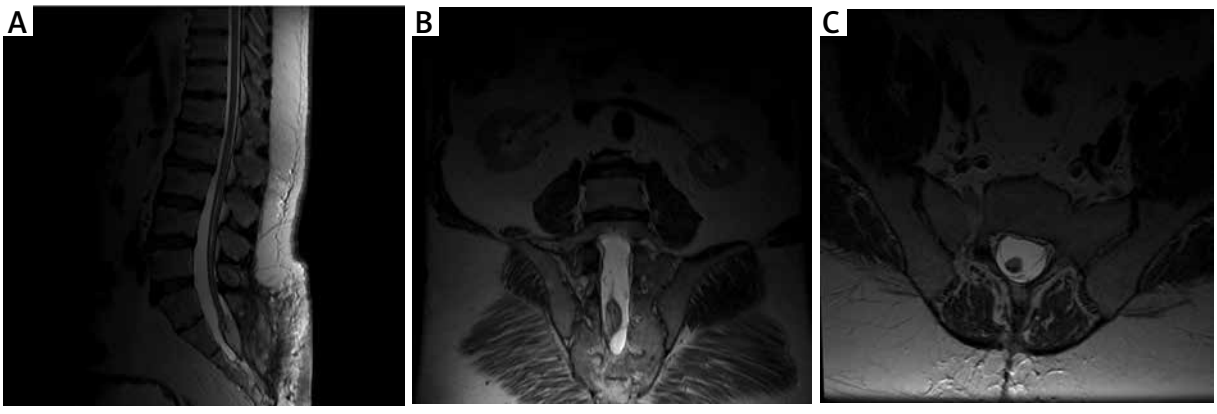

Figure 5. MRI scan at 12 months after surgery in 2 patients. **A** – MR T2 examination, postoperatively; visible postoperative wound, partially removed lipoma. **B** – MR T2 examination, postoperative coronal sections; remaining part of the adipoma is visible. **C** – MR T2 examination, postoperative axial sections

Results

Molecular evaluation of CSF

Cerebrospinal fluid aspirated several times was subjected to microbiological analysis, with negative results each time.

Alteration of gene expression profile determined by RTqPCR technique

Changes in the expression profile of analysed genes were presented in Supplementary Table S1 (https://links.lww.com/). Regardless of the observation time, overexpression was observed for all evaluated transcripts in the test samples compared to the control. However, gene expression in the samples obtained during the neurosurgery (time 0) was at a similar level as in the control. In contrast, significant increases in the transcriptional activity of the genes evaluated were observed on subsequent days of observation (days 1, 7, and 10), with the greatest changes observed for MMPs and vascular endothelial growth factor A–D (VEGF-A–D; $p < 0.05$). Changes in the expression of analysed genes were presented in Table 1.

Discussion

Amongst patients referred to and treated by urologists and general practitioners, a small group of patients has undiagnosed TCS. This necessitates an MRI scan to detect the condition, which is not easy due to the rarity of the disease, especially in adulthood [27, 28].

TCS requires surgical treatment, consisting of transection of the terminal strand and partial or total resection of the associated terminal strand lesion using an operating microscope and neuromonitoring, which greatly improves patient outcomes [29–35].

Yamada *et al.* demonstrated on a cat model that, with uniform traction on the spinal cord, different spinal cord segments elongate to different degrees, with the distal segments of the spinal cord being most vulnerable to elongation. This explains the appearance of characteristic neurological symptoms, which are a manifestation of decreased oxygen metabolism in the stretched segments of the spinal cord. Evoked potentials are also decreased, and after the reduction of traction they returned to normal except for the evoked potentials of interneurons [36]. Yamada *et al.* presented a division of the operated patients into three groups. The group with slight to moderate traction on the cord achieved full recovery after 2–4 weeks; in the third group, patients recovered partially only [37].

The most common complication after surgical treatment is subcutaneous fluid collection, which is treated (as in the case of the presented patients) with a series of punctures and evacuation of CSF or may require dura mater plication. The rarer complications include surgical wound infection, fluid from the surgical wound, epidural hematoma, or neurological complications, for example, impaired dorsiflexion of the foot or worsening of bladder dysfunction. In most studies of TCS, full recovery of the lost function is rare, with a particularly poor prognosis for sphincter function; surgical treatment is effective for pain and sensory dysfunction [1, 14, 38, 39].

In our study, we first analysed the expression pattern of 22 mRNAs associated with wound healing. The genes were selected based on the available literature [20, 21, 24–26]. The process of wound healing is multistage and begins with the formation of an aggregate at the wound site from platelets, which are a source of cytokines, primarily TGF-β, resulting in the conversion of fibrinogen into fibrin, which forms a temporary scaffold into which neutrophils, macrophages, mast cells, a source of cytokines and growth factors, invade within 48 h. Then, in the proliferative phase, the synthesis of collagen fibres and influx of fibroblasts are noted. Angiogenesis begins at the moment of endothelial cell migration to the fibrin matrix, during which an increase in the activity of TGF-β, VEGF, and FGF is noted, stimulating the formation of new blood vessels [40, 41].

During our observation, the greatest changes were observed in TGF-β, VEGF, MMP, transforming growth factor α (TGF-α), genes encoding proteins involved in the first stages of wound healing, accompanied by intensive angiogenesis, which enables the influx of nutrients and oxygen at the wound site and its healing. Nevertheless, an increase in the expression of genes encoding collagen, which plays a key role in the proliferative phase of wound healing, can also be observed. Considering that molecular changes precede phenotypic changes [42, 43], evaluation of changes in the expression of our selected genes can be used to monitor and predict the process of wound healing and scar formation, which occurred in our cases at 19 and 20 days after surgery.

Our work has strengths and weaknesses. The undoubted value of the study is the evaluation of changes in the expression profile of genes involved in wound healing during the 14-day follow-up. It is reasonable to perform molecular analysis on a larger number of patients with TCS; however, due to the rarity of this disease in the adult group, it may be very difficult. One potential solution would be to perform a multicentre follow-up, which could allow increasing the group size.

Given the rarity and uncharacteristic pattern of symptoms, the diagnosis of TCS can be very difficult, in which case MRI is crucial. Surgical treatment using microsurgical techniques and neuromonitoring is an effective method of stopping the progression of the disease and relieving patients from bothersome symptoms.

Acknowledgments

The study was conducted according to the guidelines of the Declaration of Helsinki. Approval of the Bioethi-

Table 1. Differences in the expression pattern of genes related to the wound healing process during the observation period

mRNA	0 day	1 day	7 days	10 days	$p < 0.05$
TGF-β1	(+) 1.42 (1.41;1.42)	(+)4.53 (4.51; 4.55)	(+)32.20 (32.19; 32.21)	(+)29.98 (29.97; 30.00)	0.021[A] $p < 0.0001$[B,C,D,E] $p > 0.05$[F]
TGF-β2	(+)1.07 (1.03;1.09)	(+)5.03 (5.00; 5.07	(+)23.20 (23.19; 23.20)	(+)23.05 (23.02; 23.09)	0.0014[A] $p < 0.0001$[B,C,D,E] $p > 0.05$[F]
TGF-β3	(+)1.22 (1.20; 1.23)	(+)5.14 (5.11; 5.15)	(+)29.09 (29.08; 29.09)	(+)32.95 (32.93; 32.97)	0.0012[A] $p < 0.0001$[B,C,D,E] $p > 0.05$[F]
VEGF-A	(+)1.32 (1.31; 1.32)	(+)12.82 (12.81; 12.82)	(+)21.10 (21.09; 21.11)	(+)27.19 (27.18; 27.20)	$p < 0.0001$[B,C,D,E] 0.009[F]
VEGF-B	(+)1.18 (1.12; 1.23)	(+)12.86 (12.80; 12.92)	(+)121.05 (121.03; 121.08)	(+)99.65 (99.93; 99.66)	$p < 0.0001$[B,C,D,E] 0.021[F]
VEGF-C	(+)1.02 (-.1.01; 1.02)	(+)11.62 (11.60; 11.63)	(+)176.43 (176.25; 177.00)	(+)145.98 (145.97; 145.99)	$p < 0.0001$[B,C,D,E] 0.009[F]
VEGF-D	(+)1.14; (1.12; 1.15)	(+)16.22 (16.20; 16.22)	(+)156.82 (156.80; 156.88)	(+)100.11 (100.10; 100.12)	$p < 0.0001$[B,C,D,E] 0.006[F]
MMP-2	(+)1.09 (1.08; 1.09)	(+)21.04 (21.02; 21.09)	(+)87.98 (87.97; 87.99)	(+)23.62 (23.61; 23.65)	$p < 0.0001$[A,B,C,D] $p > 0.05$[E], 0.005[F]
MMP-8	(+)1.04 (1.00; 1.08)	(+)18.54 (18.53; 18.55)	(+)83.12 (83.10; 83.13)	(+)13.83 (13.81; 13.84)	$p < 0.0001$[A,B,C,D] 0.034[E], 0.005[F]
MMP-9	(+)1.13 (1.12; 1.14)	(+)21.83 (21.80; 21.85)	(+)45.91 (45.90; 45.92)	(+)21.05 (21.04; 21.06)	$p < 0.0001$[A,B,C,D] $p > 0.05$[E], 0.012[F]
MMP-7	(+)1.22 (1.21; 1.23)	(+)19.11 (19.10; 19.12)	(+)35.02 (35.00; 35.03)	(+)12.11 (12.10; 12.13)	$p < 0.0001$[A,B,C,D] 0.022[E]
MMP-13	(+)1.22 (1.22; 1.23)	(+)31.02 (30.99; 31.06)	(+)98.20 (98.19; 98.22)	(+)22.51 (22.50; 22.54)	$p < 0.0001$[A,B,C,D] 0.018[E,F]
TNF- α	(+)1.72 (1.71; 1.74)	(+)21.12 (21.11; 21.27)	(+)34.53 (34.52; 34.56)	(+)23.99 (23.97; 24.00)	$p < 0.0001$[A,B,C,D] $p > 0.05$[E], 0.003[F]
IL-1β	(+)1.09 (1.08; 1.10)	(+)18.45 (18.41; 18.49)	(+)41.28 (4122; 41.32)	(+)22.89 (22.89; 22.91)	$p < 0.0001$[A,B,C,D] $p > 0.05$[E], 0.015[F]
FGF-2	(+)1.12 (1.11; 1.13)	(+)17.93 (17.92; 17.94)	(+)23.98 (23.98; 23.99)	(+)11.98 (11.97; 11.99)	$p < 0.0001$[A,B,C,D] 0.037[E], 0.0041[F]
EFG	(+)1.23 (1.22; 1.23)	(+)12.03 (12.01; 12.05)	(+)10.87 (10.86; 10.88)	(+)12.12 (12.10; 12.13)	$p < 0.0001$[A,B,C,D] $p > 0.05$[E,F]
COL1A1	(+)1.11 (1.10;1.12)	(+)5.47 (5.45; 5.51)	(+)3.98 (3.96; 4.02)	(+)10.34 (10.33; 10.35)	0.0031[A] $p < 0.0001$[B,C] 0.0412[D], 0.0026[E], 0.002[F]
COL1A2	(+)1.23 (1.21; 1.24)	(+)5.99 (5.99; 6.01)	(+)10.24 (10.22; 10.25)	(+)13.76 (13.75; 13.77)	0.0033[A] $p < 0.0001$[B,C,D] $p > 0.05$[F]
COL5A1	(+)1.21 (1.19; 1.23)	(+)4.12 (4.11; 4.13)	(+)10.32 (10.30; 10.33)	(+)16.73 (16.71; 16.74)	0.0049[A] $p < 0.0001$[B,C,D,E] 0.025[F]
TGF-α	(+)1.01 (1.00; 1.02)	(+)7.89 (7.87; 7.90)	(+)43.91 (43.89; 43.92)	(+)32.04 (32.02; 32.05)	$p < 0.0001$[A,B,C,D,E] 0.041[F]
IGF1	(+)1.21 (1.24; 1.20)	(+)11.01 (10.99; 11.02)	(+)19.93 (19.92; 19.94)	(+)22.12 (22.11; 22.14)	$p < 0.0001$[A,B,C,D] $p > 0.05$[F], 0.0011[E]
KGF-2	(+)1.09 (1.08; 1.10)	(+)6.17; (6.16; 6.18)	(+)15.09 (15.02; 15.11)	(+)41.45 (41.42; 41.51)	0.0019[A] $p < 0.0001$[B,C,D,E] 0.026[F]

TGF-β1 – transforming growth factor β1. TGF-β2 – transforming growth factor β2, TGF-β3 – transforming growth factor β3, VEGF-A – vascular endothelial growth factor A, VEGF-B – vascular endothelial growth factor B, VEGF-C – vascular endothelial growth factor C, VEGF-D – vascular endothelial growth factor D, MMP-2 – metalloproteinase 2, MMP-7 – metalloproteinase 7, MMP-8 – metalloproteinase 8, MMP-13 – metalloproteinase 13, TNF-α – tumor necrosis factor α, IL-1β – interleukin 1 β, FGF2 – fibroblast growth factor 2, EGF – epidermal growth factor, COL1A1 – α1 type I collagen, COL1A2 – α2 type I collagen, COL5A1 – α5 type I collagen, TGF-α – transforming growth factor α, IGF1 – insulin growth factor 1, KGF2 – keratinocyte growth factor 1, (+) – upregulated vs. control, (–) – downregulated vs. control, [A]statistically significant differences in gene expression between day 0 and 1 (post-hoc Dunn's test; p < 0.05), [B]statistically significant differences in gene expression between day 0 and 7 (post-hoc Dunn's test; p < 0.05), [C]statistically significant differences in gene expression between day 0 and 10 (post-hoc Dunn's test; p < 0.05), [D]statistically significant differences in gene expression between day 1 and 7 (post-hoc Dunn's test; p < 0.05), [E]statistically significant differences in gene expression between day 1 and 10 (post-hoc Dunn's test; p < 0.05), [F]statistically significant differences in gene expression between day 7 and 10 (post-hoc Dunn's test; p < 0.05); Median (lower quartile; upper quartile).

cal Committee operating at the Regional Medical Chamber in Krakow was obtained for this study (no. 162/KBL/OIL/2021). Informed consent was obtained from all subjects involved in the study. The data used to support the findings of this study are included in the article. The data will not be shared due to the third-party rights and commercial confidentiality.

Conflict of interest

The authors declare no conflict of interest.

References

1. Agarwalla PK, Dunn IF, Scott RM, Smith ER. Tethered cord syndrome. Neurosurg Clin North Am 2007; 18: 531-47.
2. O'Connor KP, Smitherman AD, Milton CK, et al. Surgical treatment of tethered cord syndrome in adults: a systematic review and meta-analysis. World Neurosurg 2020; 137: e221-41.
3. Chatterjee S, Rao K. Missed limited dorsal myeloschisis: an unfortunate cause for recurrent tethered cord syndrome. Child's Nerv System 2015; 31: 1553-7.
4. Jones V, Wykes V, Cohen N, et al. The pathology of lumbosacral lipomas: macroscopic and microscopic disparity have implications for embryogenesis and mode of clinical deterioration. Histopathology 2018; 72: 1136-44.
5. Blount JP, George TM, Koueik J, Iskandar BJ. Concepts in the neurosurgical care of patients with spinal neural tube defects: an embryologic approach. Birth Defects Res 2019; 111: 1564-76.
6. Eagles ME, Gupta N. Embryology of spinal dysraphism and its relationship to surgical treatment. Canad J Neurol Sci 2020; 47: 736-46.
7. Pang D, Wilberger JE. Tethered cord syndrome in adults. J Neurosurg 1982; 57: 32-47.
8. Iskandar BJ, Fulmer BB, Hadley MN, Oakes WJ. Congenital tethered spinal cord syndrome in adults. Neurosurg Focus 2001; 10: e7.
9. Gao J, Kong X, Li Z, et al. Surgical treatments on adult tethered cord syndrome: a retrospective study. Medicine 2016; 95: e5454.
10. Sysoev K, Tadevosyan A, Samochernykh K, Khachatryan W. Prognosis of surgical treatment of the tethered cord syndrome in children. Child's Nerv System 2018; 34: 305-10.
11. Abdallah A, Emel E, Abdallah BG, et al. Factors affecting the surgical outcomes of tethered cord syndrome in adults: a retrospective study. Neurosurg Rev 2018; 41: 229-39.
12. Tuite GF, Thompson DN, Austin PF, Bauer SB. Evaluation and management of tethered cord syndrome in occult spinal dysraphism: recommendations from the international children's continence society. Neurourol Urodyn 2018; 37: 890-903.
13. Steinbok P, MacNeily AE, Hengel AR, et al. Filum section for urinary incontinence in children with occult tethered cord syndrome: a randomized, controlled pilot study. J Urol 2016; 195: 1183-8.
14. Shukla M, Sardhara J, Sahu R, et al. Adult versus pediatric tethered cord syndrome: clinicoradiological differences and its management. Asian J Neurosurg 2018; 13: 264-70.
15. De Backer A. Handbook of Neurosurgery. 8th edn. Acta Chir Belg 2016; 116: 269.
16. Udayakumaran S, Rathod CT. Tailored strategies to manage cerebrospinal fluid leaks or pseudomeningocele after surgery for tethered cord syndrome. World Neurosurg 2018; 114: e1049-56.
17. Khan B, Haqqani U, Khattak RU, Hussain S. Cerebrospinal fluid leak after repair of congenital spinal pathologies, incidence and management. Pakistan J Neurol Surg 2020; 24: 253-7.
18. Novik Y, Vassiliev D, Tomycz ND. Spinal cord stimulation in adult tethered cord syndrome: case report and review of the literature. World Neurosurg 2019; 122: 278-81.
19. Guppy KH, Silverthorn JW. Spinal cord herniation after cervical corpectomy with cerebrospinal fluid leak: case report and review of the literature. World Neurosurg 2017; 100: 711-e7.
20. Lichtman MK, Otero-Vinas M, Falanga V. Transforming growth factor beta (TGF-β) isoforms in wound healing and fibrosis. Wound Repair Regen 2016; 24: 215-22.
21. Gilbert RW, Vickaryous MK, Viloria-Petit AM. Signalling by transforming growth factor beta isoforms in wound healing and tissue regeneration. J Develop Biol 2016; 4: 21.
22. Bao P, Kodra A, Tomic-Canic M, et al. The role of vascular endothelial growth factor in wound healing. J Surg Res 2009; 153: 347-58.
23. Broekman W, Amatngalim GD, de Mooij-Eijk Y, et al. TNF-α and IL-1β-activated human mesenchymal stromal cells increase airway epithelial wound healing in vitro via activation of the epidermal growth factor receptor. Respir Res 2016; 17: 3.
24. Ayuk SM, Abrahamse H, Houreld NN. The role of matrix metalloproteinases in diabetic wound healing in relation to photobiomodulation. J Diabetes Res 2016; 2016: 2897656.
25. Hingorani DV, Lippert CN, Crisp JL, et al. Impact of MMP-2 and MMP-9 enzyme activity on wound healing, tumor growth and RACPP cleavage. PLoS One 2018; 13: e0198464.
26. Mathew-Steiner SS, Roy S, Sen CK. Collagen in wound healing. Bioengineering 2021; 8: 63.
27. Wang J, Zhou Q, Fu Z, et al. MRI evaluation of fetal tethered-cord syndrome: correlation with ultrasound findings and clinical follow-up after birth. Clin Radiol 2021; 76: 314-e1.
28. Menezes AH, Seaman SC, Howard III MA, et al. Tethered spinal cord syndrome in adults in the MRI era: recognition, pathology, and long-term objective outcomes. J Neurosurg Spine 2021; 34: 942-54.
29. Finger T, Aigner A, Depperich L, et al. Secondary tethered cord syndrome in adult patients: retethering rates, long-term clinical outcome, and the effect of intraoperative neuromonitoring. Acta Neurochirur 2020; 162: 2087-96.
30. Udayakumaran S, Nair NS, George M. Intraoperative neuromonitoring for tethered cord surgery in infants: challenges and outcome. Pediatr Neurosurg 2021; 56: 501-10.
31. Udayakumaran S, Karthika KS, Nair NS, et al. Prognostication of the neurological outcome of tethered cord based on intraoperative neuromonitoring findings: how close can we get? Br J Neurosurg 2021; 1–9. DOI: 10.1080/02688697.2021.1940855.
32. Kobets AJ, Oliver J, Cohen A, et al. Split cord malformation and tethered cord syndrome: case series with long-term follow-up and literature review. Child's Nerv System 2021; 37: 1301-6.
33. Michael MM, Garton AL, Kuzan-Fischer CM, et al. A critical analysis of surgery for occult tethered cord syndrome. Child's Nerv System 2021; 37: 3003-11.
34. McVeigh LG, Anokwute MC, Belal A, et al. Spinal column shortening for secondary tethered cord syndrome:

radiographic, clinical, patient-reported, and urodynamic short-term outcomes. J Neurosurg Pediatr 2021; doi: 10.3171/2020.11.PEDS20847.
35. Seki T, Hida K, Yano S, et al. Surgical outcome of children and adolescents with tethered cord syndrome. Asian Spine J 2016; 10: 940.
36. Yamada S, Iacono RP, Andrade T, et al. Pathophysiology of tethered cord syndrome. Neurosurg Clin N Am 1995; 6: 311-23.
37. Yamada S, Won DJ, Yamada SM. Pathophysiology of tethered cord syndrome: correlation with symptomatology. Neurosurg Focus 2004; 16: E6.
38. Geyik M, Alptekin M, Erkutlu I, et al. Tethered cord syndrome in children: a single-center experience with 162 patients. Childs Nerv Syst 2015; 31: 1559-63.
39. Hou Y, Sun J, Shi J, et al. Clinical evaluation of an innovative operative procedure in the treatment of the tethered cord syndrome. Spine J 2018; 18: 998-1004.
40. Goldman R. Growth factors and chronic wound healing: past, present, and future. Adv Skin Wound Care 2004; 17: 24-35.
41. Deonarine K, Panelli MC, Stashower ME, et al. Gene expression profiling of cutaneous wound healing. J Transl Med 2007; 5: 11.
42. Szczepanowski Z, Grabarek BO, Boroń D, et al. Microbiological effects in patients with leg ulcers and diabetic foot treated with Lucilia sericata larvae. Int Wound J 2022; 19: 135-43.
43. Michalska-Bańkowska A, Wcisło-Dziadecka D, Grabarek B, et al. Variances in the mRNA expression profile of TGF-β 1–3 isoforms and its TGF-βRI–III receptors during cyclosporin a treatment of psoriatic patients. Adv Dermatol Allergol 2018; 35: 502-9.